

MASS PREDICTIONS OF ATOMIC NUCLEI IN THE INFINITE NUCLEAR MATTER MODEL*

R. C. NAYAK¹ and L. SATPATHY²

1. *Department of Physics, Berhampur University,*

Berhampur-760 007, India, EMAIL: rcnayak00@yahoo.com and

2. *Institute of Physics, Bhubaneswar-751 005, India. Email: satpathy@iopb.res.in*

We present here the mass excesses, binding energies, one- and two- neutron, one- and two- proton and α -particle separation energies of 6727 nuclei in the ranges $4 \leq Z \leq 120$ and $8 \leq A \leq 303$ calculated in the infinite nuclear matter model. Compared to our predictions of 1999 mass table, the present ones are obtained using larger data base of 2003 mass table of Wapstra and Audi and resorting to higher accuracy in the solutions of the η -differential equations of the INM model. The local energy η 's supposed to carry signature of the characteristic properties of nuclei are found to possess the predictive capability. In fact η -systematics reveal new magic numbers in the drip-line regions giving rise to new islands of stability supported by relativistic mean field theoretic calculations. This is a manifestation of a new phenomenon where shell-effect overcomes the instability due to repulsive components of the nucleon-nucleon force broadening the stability peninsula. The two-neutron separation energy-systematics derived from the present mass predictions reveal a general new feature for the existence of islands of inversion in the exotic neutron-rich regions of nuclear landscape, apart from supporting the presently known islands around ^{31}Na and ^{62}Ti . The five global parameters representing the properties of infinite nuclear matter, the surface, the Coulomb and the pairing terms are retained as per our 1999 mass table. The root-mean-square deviation of the present mass-fit to 2198 known masses is 342 keV, while the mean deviation is 1.3 keV, reminiscent of no left-over systematic effects. This is a substantive improvement over our 1999 mass table having rms deviation of 401 keV and mean deviation of 9 keV for 1884 data nuclei.

* This is a briefly enhanced version of the article just published in *Atom. Data and Nucl. Data Tables* 98(2012)213-719.

I. INTRODUCTION

Mass formulas always occupy the center-stage in the research arena of nuclear physics. Traditionally mass formulas have been developed using the two main features of nuclear dynamics, namely, the liquid drop and the shell features. The liquid drop has been the mainstay of nuclear physics since its introduction by Weizsacher and Bethe in 1930s. The liquid - supposed to represent the nuclear matter composed of the nucleus - is a classical one, although in reality it is a quantum liquid consisting of interacting many-fermionic system. At macroscopic level the classical liquid picture has been most useful as a reference model. However it has given rise to some discomfitures, the notable being the $r_0 - paradox$ [1, 2] i.e., the discrepancy between the density determined by it through the fit to nuclear masses and the actual density measured through electron scattering on heavy nuclei. In the infinite nuclear matter (INM) model[3-6], the classical liquid drop is replaced by an INM sphere characterizing the interacting many-fermionic liquid. Further the model is based on the Extended Hugenholtz-Van Hove theorem[4, 7] of many-body theory, and therefore takes into account the shell and the liquid-drop features nonperturbatively.

The first mass table based on this model was published[5] in 1988 with predictions of 3481 nuclei. The far-off nuclei in the drip-line regions could not be included because of accumulated error resulting from imprecise solution of η -equation. Further development in the INM model was achieved by using better definition of Fermi energies leading to perfect decoupling[8, 9] of the finite-size terms like surface and Coulomb from the infinite-nuclear-matter terms characterized by volume and asymmetry. This led to the determination[8, 9] of the saturation properties of nuclear matter i.e., the density, the binding energy per nucleon and the incompressibility from nuclear masses and thereby resolving[8, 9] the $r_0 - paradox$. Thus the basic objective of the INM model was achieved. Further for the successful long-range prediction of nuclear masses, an interactive network extending over the entire nuclear chart was devised[6] for better determination of the local energy η . This procedure yielded multiple values of η for a given nucleus whose ensemble-average was carried out to obtain its unique value. With these improvements, reliable prediction of nuclear masses up to drip-line could be made and the second mass table containing the data for 7208 nuclei was published[6] in 1999.

Up to 1999 our concern was directed towards the long-standing problem of the determi-

nation of the saturation properties of nuclear matter and its incompressibility from nuclear masses[8, 9]. Once this objective was fulfilled we concentrated on the study of properties of local energy η , a crucial element in the INM model. η embodies all the characteristic properties of a nucleus, and therefore carries its finger-print. The η 's determined in our 1999 mass predictions were analyzed as a function of neutron number N for a given proton number Z revealing[10] Gaussian structure for the well-known closed-shell nuclei in the valley of stability and similar pattern for some nuclei in the far-off drip-line regions[11]. On the basis of such revelations, new neutron magic numbers 100, 150, 164 and proton magic number 78 and weakly proton magic number 62 and 90 were predicted[11] designating new islands of stability around ^{162}Sm , ^{228}Pt and ^{254}Th reaffirmed through microscopic study[11] in the Relativistic Mean Field (RMF) theory and Strutinsky Shell-Correction calculations. This is suggestive of a new phenomenon where shell stabilizes the instability due to repulsive components (triplet-triplet, singlet-singlet) of nucleon-nucleon interaction, complementary to the phenomenon of fission isomers and super-heavy elements in which repulsive coulomb instability is overcome by the same. While the latter elongates the stability peninsula, the former broadens it. In another development, comparative study[12–14] of the predictive ability of different mass formulas carried out with respect to a reference mass formula shows random divergences without any common trend. This raises the question about predictive ability of mass formulas and their possible use as guidelines for theoretical and experimental study in unknown regions. Taking the masses calculated in the microscopic study employing RMF theory as reference masses, it is shown[15] that the divergence disappears yielding common trend for the prediction of all mass formulas. Similar trend is also observed[15] when masses predicted in our 1999 mass table are used as reference. This success could be attributed to the very structure of the INM model equations. It is identified that this mass formula is written down in terms of differential equations. It is a well recognized fact that predictive ability is intrinsic in any theory formulated in terms of differential equations like that of Newton, Schrodinger and Dirac etc. involving rate of change of physical variables. This feature of the INM model was not specifically recognized or perceived so far. We had implicitly articulated that η 's of unknown regions were obtained by some kind of extrapolation, which was somewhat misleading.

In view of the above developments after 1999, and quite importantly availability of large number of new measurement of mass of unknown nuclei in the intervening period, prompted

us to make a fresh and probably the final mass table. Addition of 314 newly measured data to the already used 1884 masses in our 1999 mass table, and more precision solution of η -differential equation being possible has resulted in the reliable prediction of masses covering up to drip-line regions with rms deviation of 342 keV and mean deviation of 1.3 keV. This is a substantive improvement over our earlier result of 1999 for 1884 mass data with rms deviation of 401 keV and mean deviation of 9 keV.

II. THE INFINITE NUCLEAR MATTER MODEL

Although the INM model is well-known and described in several papers [3, 5, 6, 9], for easy reference and completeness, a brief account is presented here. The INM model is based on quantum-mechanical infinite nuclear matter rather than the classical liquid-drop used in the traditional Bethe-Weizsacker (BW) type mass formulas. In this model, the ground-state energy $E^F(A, Z)$ of a nucleus with neutron number N , proton number Z , mass number A and asymmetry $\beta = (N - Z)/(N + Z)$ is considered equivalent to the energy of a perfect sphere made up of infinite nuclear matter at ground-state plus the residual characteristic energy called the local energy η . η mainly consists of energies due to shell, deformation and diffuseness etc., which are intrinsic characteristic properties of a given nucleus and can be considered as its finger-print. Thus a nucleus possess two categories of properties, namely, the global one represented by the INM sphere and the individualistic one by $\eta(A, Z)$. So

$$E^F(A, Z) = E^S(A, Z) + \eta(A, Z) \quad (1)$$

with

$$E^S(A, Z) = E(A, Z) + f(A, Z), \quad (2)$$

where

$$\begin{aligned} f(A, Z) = & a_s^I A^{2/3} + a_C^I [Z^2 - 5(\frac{3}{16\pi})^{2/3} Z^{4/3}] A^{-1/3} \\ & + a_{ss}^I A^{2/3} \beta^2 + a_{cv}^I A^{1/3} - \delta(A, Z) \end{aligned} \quad (3)$$

denotes the finite size effects and $E(A, Z)$ is the energy of the infinite nuclear matter contained in the sphere. This sphere is hereafter referred to as the INM sphere, and the superscript I stands for the INM nature of the coefficients. Here a_s^I , a_C^I , a_{ss}^I and a_{cv}^I are the surface,

Coulomb, surface-symmetry and curvature coefficients and $\delta(A, Z)$ is the usual pairing term, given by

$$\begin{aligned}\delta(A, Z) &= +\Delta A^{-1/2} \quad \text{for even - even nuclei} \\ &= 0 \quad \text{for odd - A nuclei} \\ &= -\Delta A^{-1/2} \quad \text{for odd - odd nuclei}\end{aligned}\tag{4}$$

Eq. (1) now becomes

$$E^F(A, Z) = E(A, Z) + f(A, Z) + \eta(A, Z)\tag{5}$$

Thus the energy of a finite nucleus is written as the sum of three distinct parts: An infinite part E , a finite part f and a local part η . All these three parts are considered distinct in the sense that each of them refers to a different characteristic of the nucleus and as such, is more or less independent of each other. Eq. (5) is our required mass formula which provides a direct link between finite nuclei to nuclear matter. Its three functions E , f and η are to be determined.

The term $E(A, Z)$ being the property of nuclear matter at the ground state, must satisfy the generalized [4] HVH theorem given by

$$\frac{E}{A} + \rho \frac{\partial(E/A)}{\partial \rho} = \frac{1}{2}[(1 + \beta)\epsilon_n + (1 - \beta)\epsilon_p].\tag{6}$$

Using Eq. (5), the INM Fermi energies ϵ_n and ϵ_p can be expressed in terms of their counterparts of finite nuclei denoted through suffix 'F' as

$$\begin{aligned}\epsilon_n &= \epsilon_n^F - (\partial f / \partial N)_Z - (\partial \eta / \partial N)_Z \\ \epsilon_p &= \epsilon_p^F - (\partial f / \partial Z)_N - (\partial \eta / \partial Z)_N\end{aligned}\tag{7}$$

where $\epsilon_n^F = (\partial E^F / \partial N)_Z$ and $\epsilon_p^F = (\partial E^F / \partial Z)_N$. Using Eqs. (5) and (7), the relation (6) can be recast as

$$\frac{E^F}{A} + \frac{\eta}{A} = \frac{1}{2}[(1 + \beta)\epsilon_n^F + (1 - \beta)\epsilon_p^F] + S(A, Z)\tag{8}$$

$$+ \frac{1}{2}[(1 + \beta)\left(\frac{\partial \eta}{\partial N}\right)_Z + (1 - \beta)\left(\frac{\partial \eta}{\partial Z}\right)_N],\tag{9}$$

where,

$$S(A, Z) = f/A - (N/A)(\partial f/\partial N)_Z - (Z/A)(\partial f/\partial Z)_N \quad (10)$$

is a function of all the finite-size coefficients a_s^I, a_c^I, a_{ss}^I and a_{cv}^I which are global in nature. As noted earlier, the local energy η refers to the individualistic characteristic of the nucleus, while the global function $S(A, Z)$ refers to the bulk properties which are global in nature. Also the above Eq. (9) does not have any coupled term involving these two functions η and S . Therefore, we make the ansatz of splitting the above equation into the following two equations.

$$\frac{E^F}{A} = \frac{1}{2}[(1 + \beta)\epsilon_n^F + (1 - \beta)\epsilon_p^F] + S(A, Z) \quad (11)$$

or equivalently

$$S(A, Z) = \frac{E^F}{A} - \frac{1}{2}[(1 + \beta)\epsilon_n^F + (1 - \beta)\epsilon_p^F] \quad (12)$$

and

$$\frac{\eta(A, Z)}{A} = \frac{1}{2}[(1 + \beta)(\partial\eta/\partial N)_Z + (1 - \beta)(\partial\eta/\partial Z)_N]. \quad (13)$$

If individually each of these Eqs. (12, 13) is satisfied, then the original Eq. (9) is satisfied. We would like to stress here that the validity of these two equations have been well demonstrated a'posteriori in numerical calculations elsewhere [3, 5, 6].

These three equations define the INM model completely; Eq. (6) determines the finite-size coefficients a_s^I and a_c^I etc. of the INM sphere, Eq. (7) determines the global parameters a_v^I and a_β^I while Eq. (8) exclusively determines the local energy η . Thus once the three functions $E(A, Z), f(A, Z)$ and $\eta(A, Z)$ are determined, the energy of the nucleus (A, Z) is obtained using the mass formula Eq. (3).

III. CALCULATION

It should be emphasized here that the above three Eqs.(6-8) exclusively determine the surface, the bulk and the local energies of a given nucleus separately. The decoupling of these three quantities provides the necessary breakthrough[8, 9] for the correct determination of their respective parameters inhibiting cross correlations amongst them. This led[8, 9] to the resolution of the $r_0 - paradox$ and determination of the saturation properties including the incompressibility of nuclear matter entirely from nuclear masses. The parameters a_s^I, a_c^I, a_{ss}^I

and a_{cv}^I characterizing the INM sphere are global in nature. The surface symmetry a_{ss}^I term cancels to the extent of 66% due to particular combination of data occurring in it. Further being a higher order term, it is quite weak compared to the principal term. Combination of these two features makes it redundant and rather symbolic at numerical level in the INM model thereby playing no significant role. We have demonstrated this through exhaustive numerical calculation in references [[8, 9]]. The same is true for the curvature a_{cv}^I term. So we have dropped these two terms. We would like to emphasize that in the INM model we have adopted the principle to determine all the parameters using exclusively the ground-state masses of nuclei only as the model is intended to predict the ground-state masses. In the BW-like mass models[16, 17] the the value of surface-symmetry coefficient a_{ss} , is usually fixed using properties other than the ground-state masses like fission barrier etc. and the curvature term is normally dropped as its coefficient cannot be determined uniquely. It is true that by dropping the surface-symmetry term in our model, isospin-dependence is exclusively taken care of by the bulk symmetry term only and any left-over isospin dependence arising from the surface-symmetry of a given nucleus is taken care of by the characteristic local energy $\eta(N, Z)$. Thus this in no way denies any loss of generality regarding explicit absence of the isospin-dependent surface-symmetry term in the INM model.

We have also made an exhaustive study to include other higher order terms like Nolen-Schiffer charge-asymmetry and proton-form factor etc., however they could not be determined uniquely using the masses and the neutron- and proton-separation energies in the framework of our model as they exactly cancel out in the INM Eq. 6(see Ref.[8, 9] for details). In BW-like mass models the coefficients of these higher order terms are fixed using properties other than the ground-state masses. They vary widely from one model to another. For example, in the Finite-Range Droplet (FRDM) model[16], the value of charge-asymmetry coefficient is 0.436 MeV while in the Finite-Range Liquid-Drop (FRLDM) model[16] its value is 0.10289 MeV. In view of such wide variation in the value of this parameter, we feel in general, that it is not desirable to assign some values to them from external considerations using properties other than the masses. Thus although their explicit representation in the INM model is untenable, however their collective effect is implicitly accounted for through the local energy *eta* being determined by solving Eq. (8) using known experimental masses. Thus we have altogether four global parameters a_v^I , a_β^I , a_s^I , a_c^I and the pairing coefficient Δ . Since these parameters are universal in nature being valid for all nuclei, they have been

meticulously determined earlier[6, 8, 9] taking experimental masses with error bar less than 60 keV to avoid pollution from other available data with higher error. With these criteria, the masses of nuclei in the valley of stability were chosen together with their neutron and proton separation energies in fitting Eq. (6) and Eq. (7). Although in the present mass table we are using extra 314 nuclei for mass predictions compared to our 1999 mass table, they are not necessarily suitable for the determination of the global parameters as they are more exotic in nature. So we have adopted the same values for the global parameters as determined for the 1999 mass table[6, 8, 9]. These values are

$$a_v^I = 16.108 \text{ MeV}$$

$$a_\beta^I = 24.06 \text{ MeV}$$

$$a_s^I = 19.27 \text{ MeV}$$

$$a_c^I = 0.7593 \text{ MeV}$$

$$\Delta = 11.505 \text{ MeV}.$$

Once the global parameters defining $E(A, Z)$ and $f(A, Z)$ are known, the empirical values of η for all known nuclei are determined using the mass formula Eq. (5). Prediction of masses of nuclei in the unknown regions amounts to predicting the η 's of such nuclei. η satisfies Eq. (13) which is a partial differential equation in (N,Z) space. Being expressed in terms of rate of change of η with N and Z, it is endowed with good predictive ability like well-known equations in Physics. With proper initial conditions given by experimental values of η in known regions, long range prediction of η s can be obtained in unknown regions by solving the Eq. (13). In all our previous publications on the INM model we have presented in detail the construction of the grid in (N, Z) space and the method of solution, which we do not feel any necessity to repeat here. However, we would like to reiterate only the ensemble averaging process which was introduced for the 1999 mass table predictions[6], which in fact was crucial for getting proper solution of the η -Eq. (8). Fixing a hexagonal grid for 58 nuclei in a given region in (N,Z) space (see Fig. 1), Eq. (8) is solved to obtain definite values of η for those nuclei. Shifting the grid in all possible directions in (N,Z,A) space, an ensemble of about 70 alternate values for a given nucleus is generated. The most probable value is then obtained by performing ensemble-averaging using the standard Gaussian weighted method given by

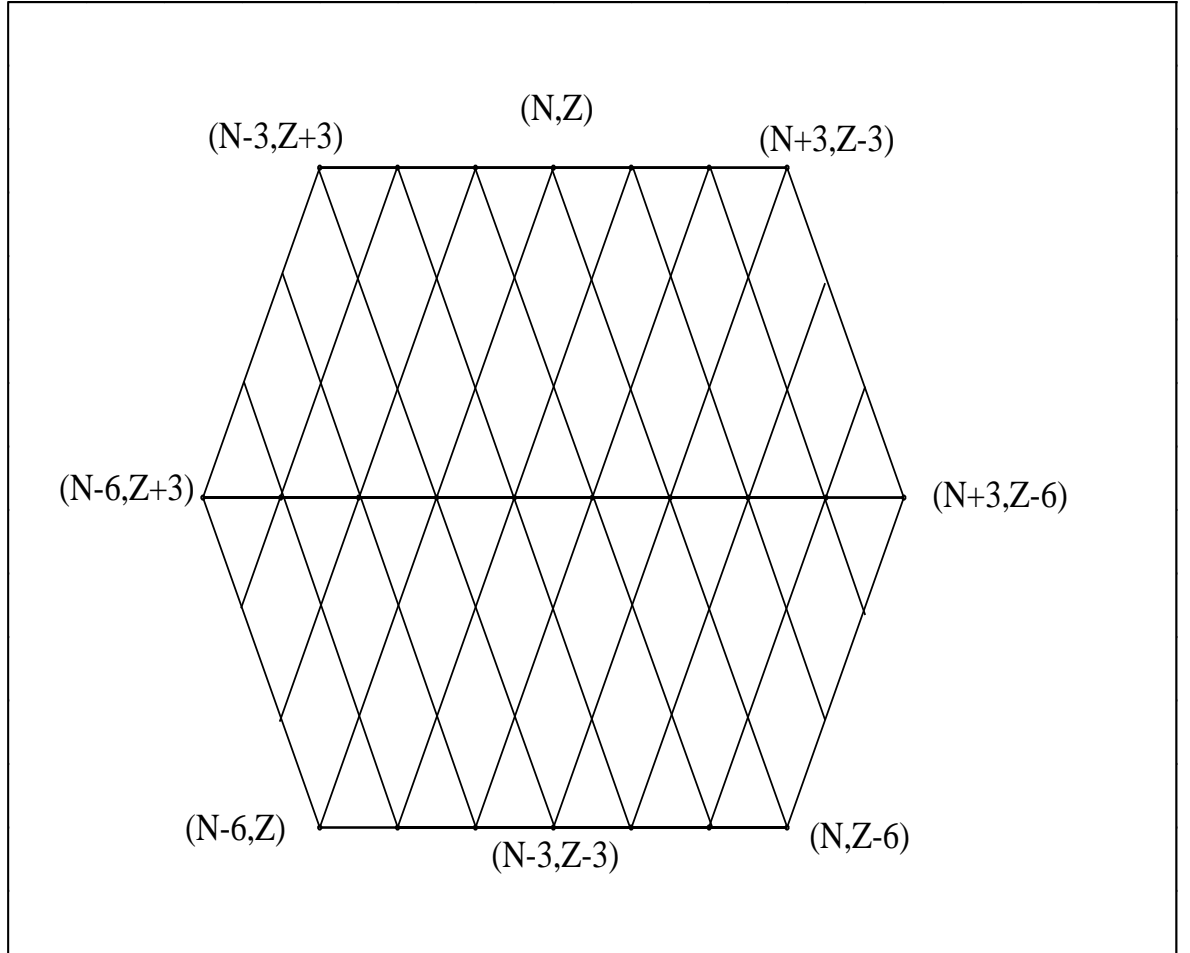


FIG. 1: The vertices in the hexagon designated by neutron and proton numbers show possible connections among the nuclei taking part in the solutions of the local energy η -equation. (13).

$$\eta = \frac{\sum_i \eta_i \exp[-((\sigma_i - \sigma_0)/\sigma_{rms})^2]}{\sum_i \exp[-((\sigma_i - \sigma_0)/\sigma_{rms})^2]}, \quad (14)$$

where σ_0 is the least of all the σ_i s for a given nucleus and σ_{rms} is the rms deviation of all the 2198 known nuclei used in the fit. Finally we use the global terms $E(A, Z)$ and $f(A, Z)$

in Eq. (3) along with the value of η so determined to predict the mass of a given nucleus in any part of the nuclear chart.

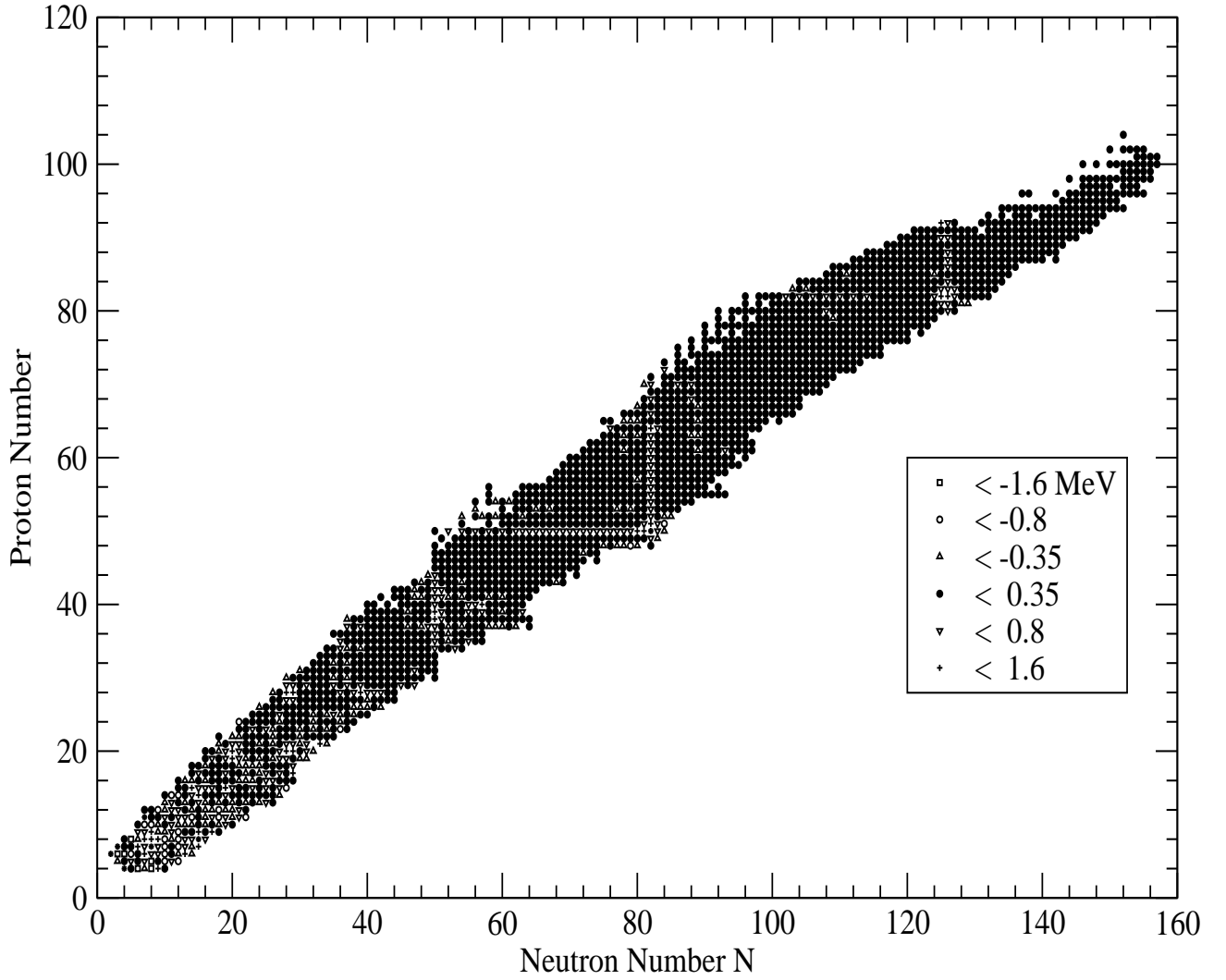


FIG. 2: Differences between the experimental (Ref.[18]) and calculated binding energy(BE) for 2198 known nuclei.

As before we observe a systematic deviation in the binding energies of $N=Z$ nuclei as a function of mass number as shown in the Fig. 2 of reference[6]. There are altogether 31

such nuclei. The binding energy systematics resemble very closely the Wigner contribution usually taken into account in the droplet-like models. As before we have taken the Wigner-like term given by $W = W_0/A\delta_{N,Z}$ as a correction to be applied for such nuclei. We have taken the value of W_0 as 32 MeV as determined before[6].

Once the global parameters and the local energies are obtained, the INM mass Eq. (3) is used to calculate the nuclear masses for the entire nuclear chart. Thus the present mass table is constructed comprising 6727 nuclei in the range $4 \leq Z \leq 120$ and $8 \leq A \leq 303$ extending up to the drip lines. It may be noted here that our present mass predictions are confined up to the drip lines and in most cases three to four steps beyond the drip lines in the nuclear landscape. We feel that this coverage of the nuclear landscape is sufficient enough for most applications both in Nuclear Physics and Astro-Physics. That is why the present mass table has 6727 mass predictions compared to 7208 in our 1999 mass table[6]. The rms deviation for the fit to 2198 data-nuclei[18] is found to be 342 keV while the mean deviation is 1.3keV.

IV. RESULTS AND DISCUSSIONS

A. General Features

To check if there is any local fluctuations in the quality of our fit, we have plotted in Fig.2 the differences between the experimental[18] binding energies (BE) and the fitted ones termed as BE residuals, in the different regions of $N - Z$ plane. The various symbols in the figure represent the magnitude of the BE residuals. It is satisfying to see that the magnitude of the residuals mostly lie within 350 keV in accord with the rms deviation of 342 keV. In Fig. 3, we have also plotted the BE residuals as a function of mass number A to study if any residual systematics are present, which would signal the deficiencies of our model. It is interesting to see that the residuals are evenly distributed around the A -axis mostly lying within 350 keV, which is well corroborated by the small mean deviation of 1.3 keV.

We would like to point out below the unique features of this mass formula which endows it with such low rms and mean deviation.

- (i) The INM model uses not only the nuclear masses like other mass models, but also additional two sets of data namely the energy differentials $(\partial E/\partial N)_Z$ and $(\partial E/\partial Z)_N$.

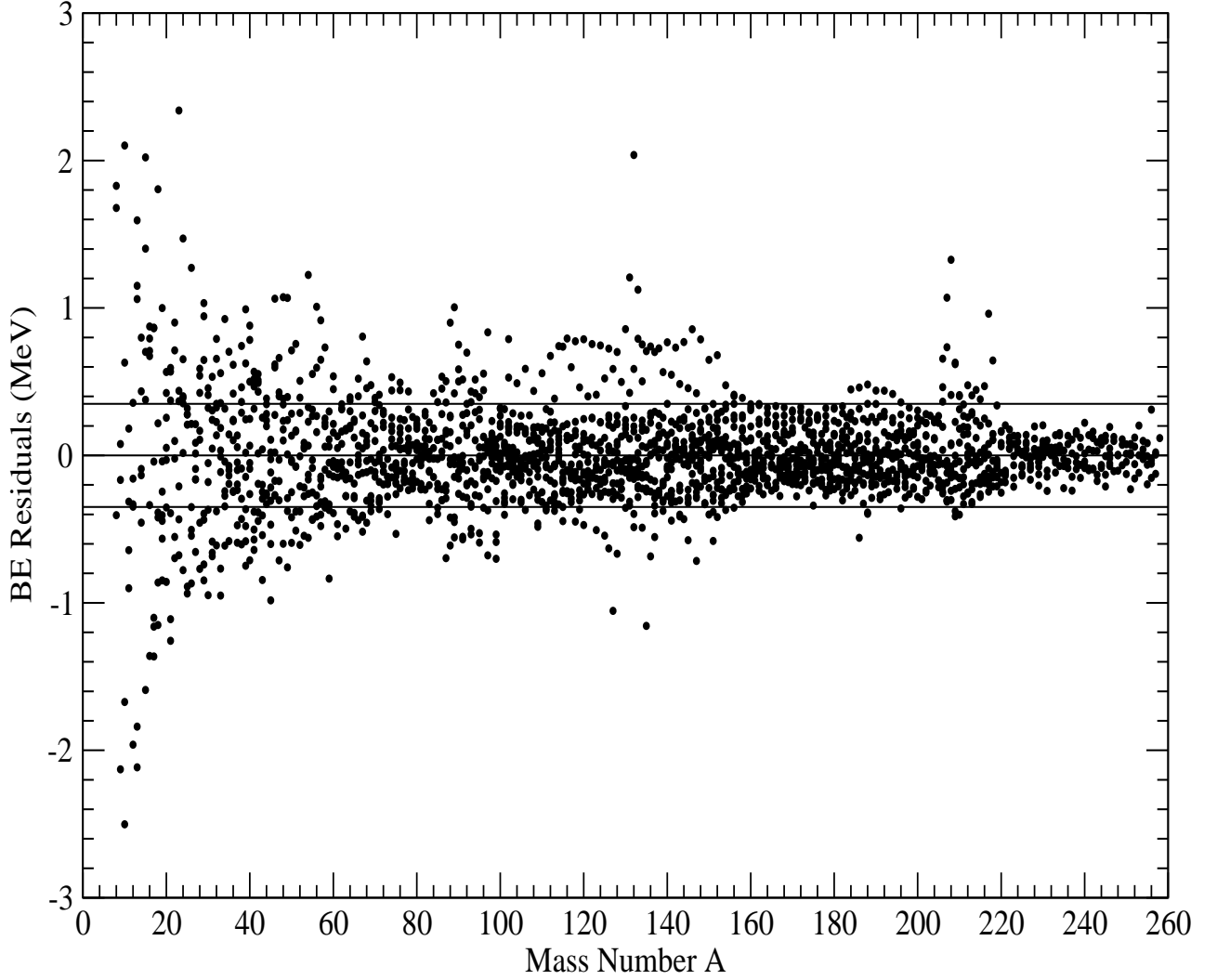


FIG. 3: The deviation as a function of mass number A of the calculated binding energies (BE) from the experimental data taken from Ref. [18] for 2198 nuclei. The two horizontal lines parallel to A -axis drawn at ± 0.35 MeV enclose most of the BE residuals.

It may be mentioned that for any function in general, all the derivatives at a point are its independent properties apart from the value of the function at that point. Thus effectively the model uses three times the mass data pertaining to three different

properties of nuclei unlike other models for fitting its parameters.

- (ii) The model uses the same set of data two times separately in solving Eqs. (6) and (7). More over in solving Eq. (8) it uses several tens of times the same set of data.
- (iii) Unlike the droplet-like mass formulas, the global parameters a_v^I and a_β^I are determined by one equation (Eq. 7) and the a_s^I and a_c^I etc. are determined by another equation (Eq. 6), which allows no cross-correlation among them thereby leading to correct values of these parameters.
- (iv) Since HVH theorem is valid for three-body and other multi-body forces, the INM model being based on it takes them implicitly into account. This is very important since three-body forces have been recognized to contribute significantly to nuclear structure and the saturation properties.

In our least-square fit, we have not included the masses of those nuclei given in the mass Table of Audi and Wapstra[18] which are not experimentally measured but estimated from systematic trends (referred to as Audi-Systematic Data). These nuclei mostly lie in the vicinity of known mass surface with relatively large error bars. There are altogether 936 such nuclei. It may be of interest to compare our predictions with these data as presented in Fig. 4. It is satisfying to note that our predictions compare well with the Audi-Systematic Data.

B. Predictive Potential of the INM model

We would like to critically examine the predictive potential of the INM model basing on two aspects; namely the structural nature of the local energy η -systematics, and comparative global analysis of the predictions of different mass models.

1. Structural Nature of η -systematics:

The key element in the INM model is the local energy η which embodies all the characteristic properties of a given nucleus, namely the shell effect, the deformation, the diffuseness etc., and possibly other unknown properties. Therefore it is expected that study of η should reveal some important features of nuclear dynamics. In such a study[10] the plot of $\eta(A,Z)$

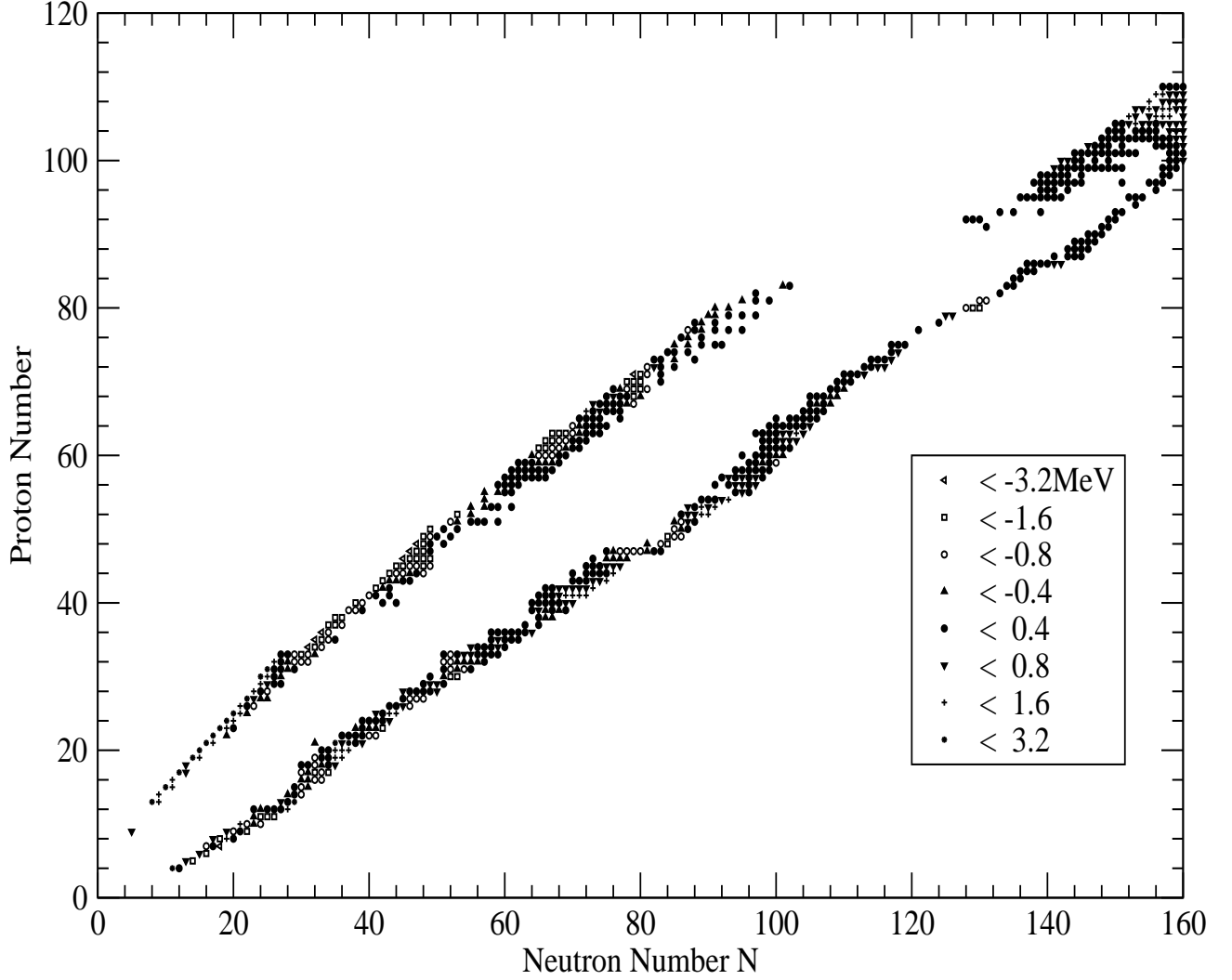


FIG. 4: Differences between binding energies (BE) of the Audi-Systematics data (Ref. [18]) and the calculated values of 936 nuclei.

as a function of N for a given Z shows Gaussian peak at shell-closures in the valley of stability. Such plots using the present empirical values of η for all the known nuclei are presented in Fig. 5, where well-defined Gaussian structures at the magic numbers 50, 82 and 126 are prominently seen. This feature is suggestive that the η -systematics in the unknown

regions may reveal new shell-closures in the neutron-rich region close to drip-line which is corroborated in the following study.

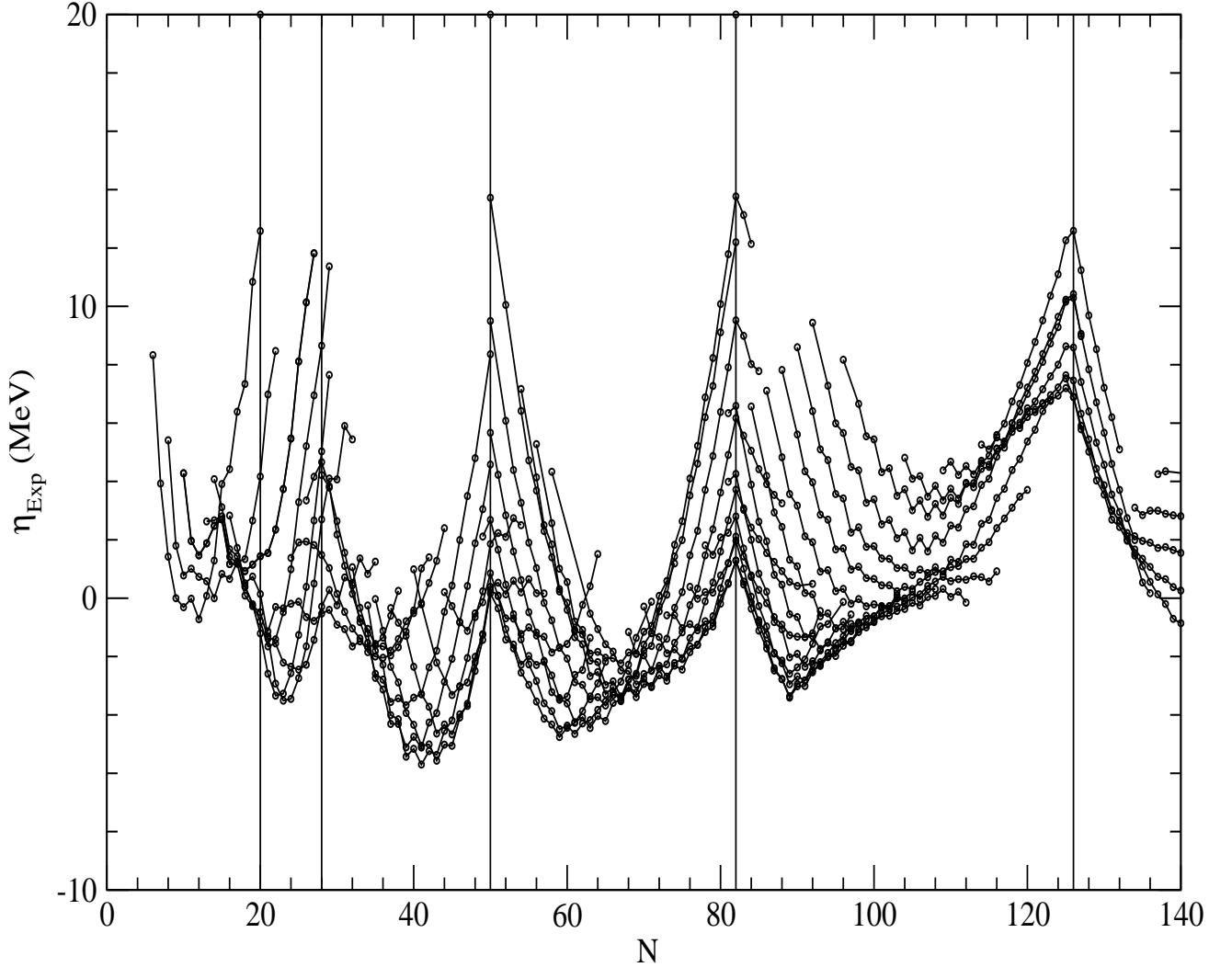


FIG. 5: Empirical values of η as functions of N for all Z showing structural nature of η -isolines. Vertical lines drawn at the Magic Numbers 20, 50, 82 and 126 and the semi-magic number 28 indicate Gaussian structure.

In 2004, we[11] have shown the predictive potential of the INM model by predicting new

neutron magic numbers 100, 150,164 and proton magic number 78 and weakly proton-magic numbers 62 and 90 along with new islands of stability around ^{162}Sm , ^{228}Pt and ^{254}Th in the drip-line regions. This prediction signals a new phenomenon where shell effect overcomes the instability due to repulsive components (triplet-triplet, singlet-singlet) of nucleon-nucleon interaction, which is complementary to the phenomena of super heavy elements and fission isomers, in which repulsive coulomb instability is overcome by the same. While the latter elongates the stability peninsula the former broadens it. This prediction was done on the basis of S_{2n} and η systematics obtained in our INM mass predictions. These results were corroborated through microscopic studies in RMF theory and Strutinsky shell correction calculations. Here we reinvestigated the same with our new mass predictions. In Fig. 6, we have plotted S_{2n} in the upper panel, η in the middle panel and the S_{2n} - differential given by $S_{2n}(N, Z) - S_{2n}(N + 2, Z)$ in the lower panel, which reaffirms our earlier result stated above. Thus the ability of the INM model for long range predictions looks promising.

2. Comparative Global Analysis of Mass Models:

Presently about 2200 nuclei are known and masses of another 5000 to 7000 nuclei have been predicted by different mass formulas. Some of them are expected to be synthesized in the RIB facilities in the coming years. Therefore the predictive ability of different mass formulas is under serious scrutiny[12–14] in the recent years. For this purpose, the predictions of different mass models [16, 19] for Sn isotopes with neutron number ranging from 45 to 110 have been compared with those of Duflo-Zucker[20] as the reference chosen for its conspicuously low rms value of 375 keV. Such studies[12–14] reveal that all mass models[16, 19] show good agreement in the known region in the valley of stability, however the predictions diverge randomly without showing any correlation as one moves away to the unknown regions on either side where experimental results are not available. This has raised serious question about the efficacy of mass formulas[16, 19] as the tools for prediction. For our discussion here we carry out such comparisons more extensively with respect to Duflo-Zucker, RMF and our present INM model predictions not only for Sn isotopes, but also for Pb and Ca isotopes. Here for a nucleus (N, Z) , the BE difference $BED_i(N, Z)$ in the model i is obtained as

$$BED_i(N, Z) = BE_i(N, Z) - BE_{ref}(N, Z) \quad (15)$$

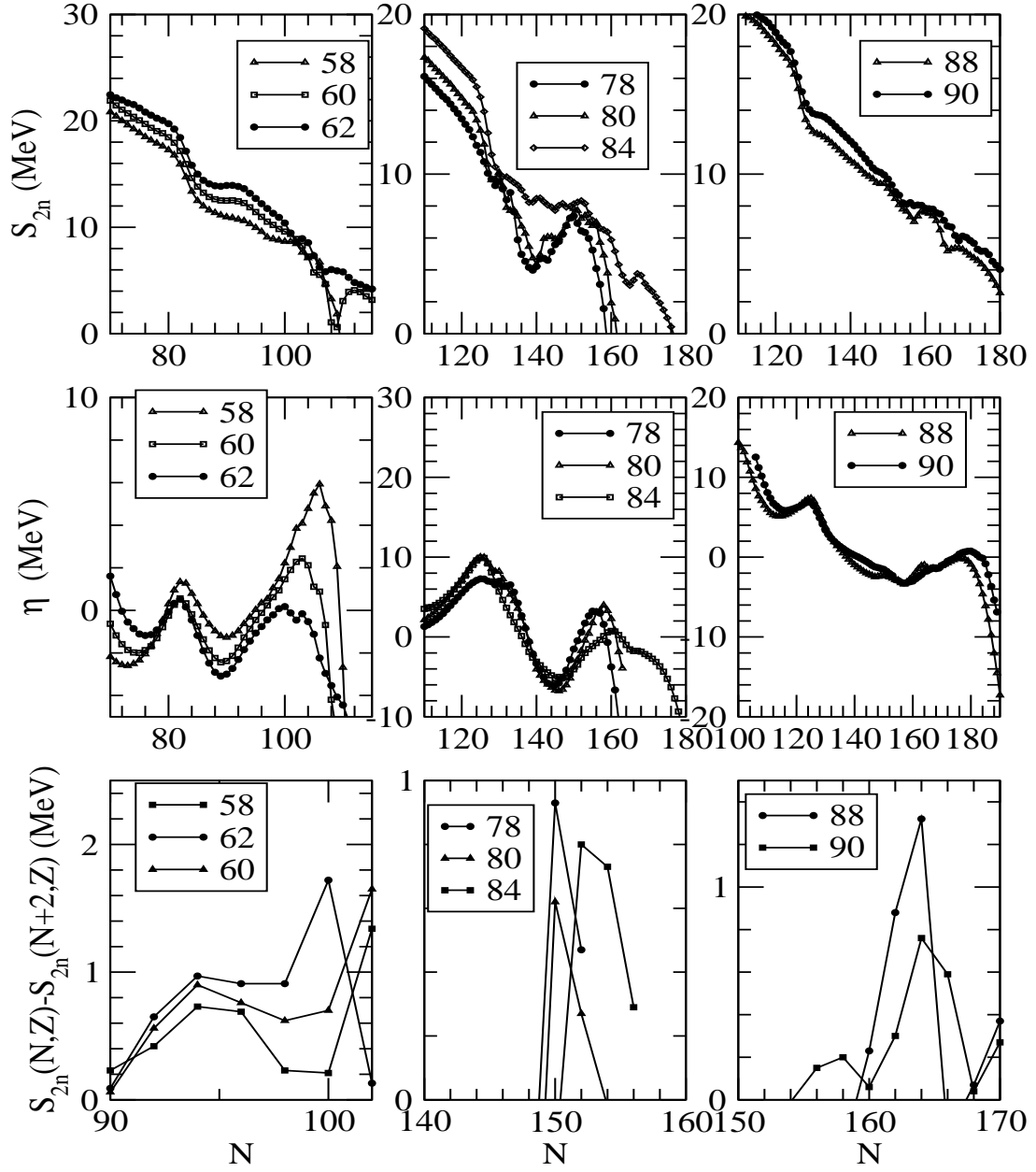


FIG. 6: S_{2n} , η and S_{2n} -differential (see text) showing occurrence of new shell-closures in ^{162}Sm , ^{228}Pt and ^{254}Th .

where $BE_i(N, Z)$ and $BE_{ref}(N, Z)$ are the predicted BEs in the mass model i and the reference mass model respectively. With Dufflo-Zucker taken as the reference model, results are plotted in Fig. 7 for the Sn, Pb and Ca isotopes separately. It can be seen that there is unanimity of all the mass models[16, 19] on good agreement with experiment in the known region in the valley of stability; however the predictions diverge as one moves away to unknown regions on either side. Since the masses of the known regions have been used in the fit by all the mass models[16, 19], the agreement with data is to be expected. What is worrying is in the unknown regions where they do not exhibit a common trend like rising and falling, but diverge without any correlation. The divergence with the same intensity is also seen when the model of Moeller and Nix et al[16] is used as the reference model in Eq. (10) as is seen in Fig. 4 of Ref.[12]. This uncorrelated divergence has raised the question about the efficacy of mass models[16, 19] as a whole[12–14]. One is constrained to think whether development of different mass models is a parameter game only without potential for reliable predictions! A probable explanation of this phenomenon may be as follows.

It is a common feature with most mass models that the degree of success varies from region to region in (N, Z) space even in known domains and may be more so in unknown domains. It is quite likely, the degree of accuracy of the predictions of a given model may not match with the corresponding ones of the reference model in the same (N, Z) domain resulting in randomness with no common trend, which appear as divergences seen in Fig. 7.

A microscopic study based on nuclear Hamiltonian may throw light on the above issue. We feel masses calculated in Relativistic Mean Field (RMF) theory can qualify to serve as a reference mass model. The popular parameter set widely used in literature with conspicuous success is the NL3 set[21]. The 7 parameters of this Lagrangian have been determined by fitting the data of ten nuclei only, and with the interaction so determined the predictions[22] of 1315 even-even nuclei give rms deviation of 2.6 MeV. It must be noted that the masses of these nuclei were not fitted unlike other models. So they should be considered as predictions in the unknown region. Therefore similar validity of this interaction in the framework of the RMF for a few hundred nuclei in the true unknown regions may be expected in a somewhat lesser scale. The BED_i 's calculated with the RMF predictions as reference for all the isotopes of Ca, Sn and Pb are shown in Fig. 8. It can be seen that for each chain of these isotopes, the predictions in the unknown regions show a common trend in general for all the mass models[16, 19], although qualitatively they differ from one another.

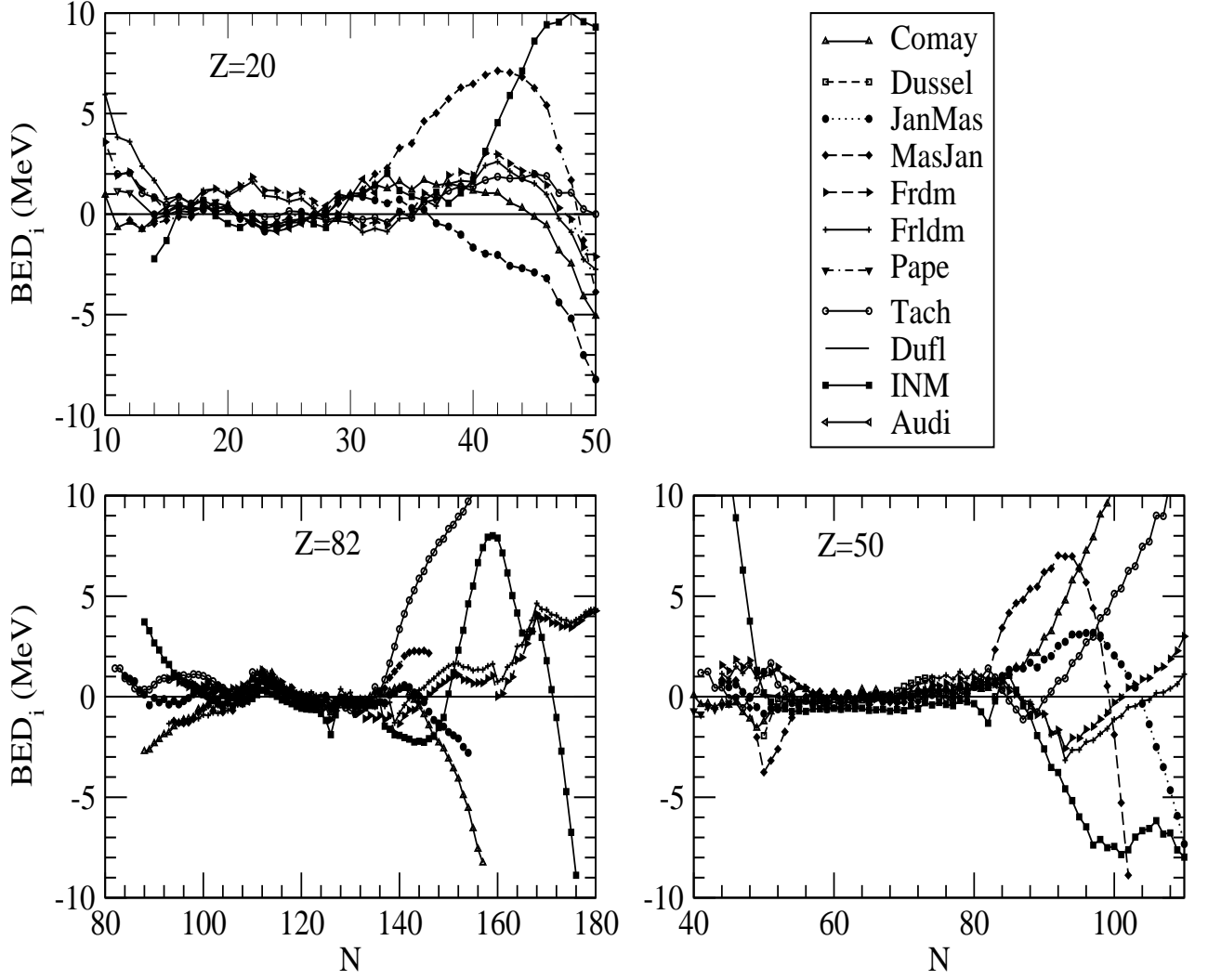


FIG. 7: Binding energy difference BED_i 's(Eq. 10) in Ca,Sn and Pb isotopes of various Mass Formula[16, 19] predictions with respect to those of Duflo-Zuker[20] as the reference.

Therefore we may conclude that the predictions of mass models in the unknown regions are not necessarily arbitrary or random but show definite trends, which therefore can be used as useful guidelines for theoretical and experimental studies. So RMF mass predictions provide a uniform substratum for the whole (N,Z) domain suitable to serve as a reference.

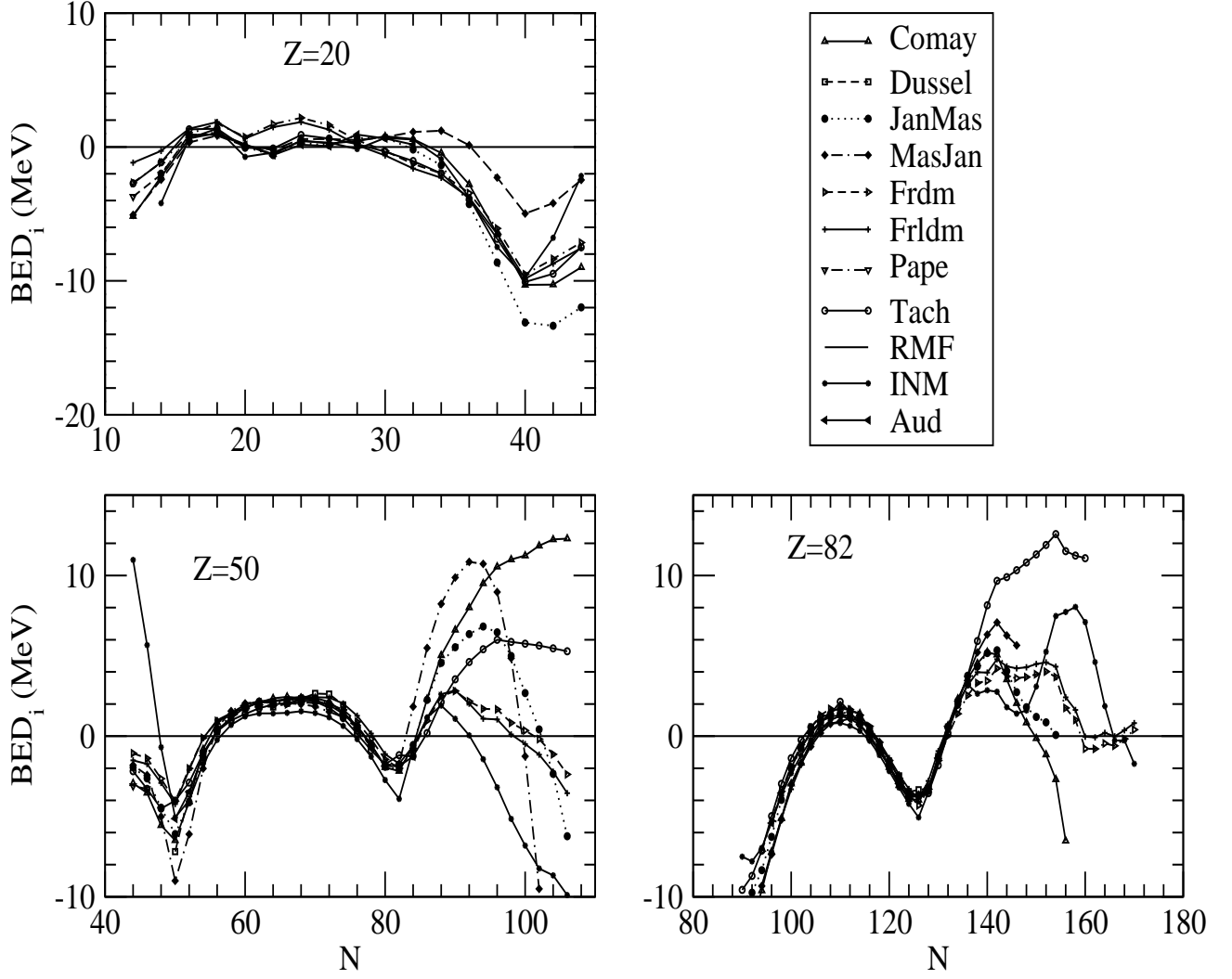


FIG. 8: Binding energy difference BED_i 's (Eq. 10) in Ca, Sn and Pb isotopes of various Mass Formula[16, 19] predictions with respect to those of RMF[22] as the reference.

Now in the context of our present mass predictions in the INM model, we use it as the reference model in Eq. (10) to calculate the BED_i 's for all those isotopes of Ca, Sn and Pb. The results so obtained are presented in Fig. 9. It is satisfying to find that no random divergences appear in the unknown regions, rather the expected common trends are seen in

all the three cases. Thus like the RMF mass predictions, INM mass predictions can also be used as substratum for suitable reference purposes. This implicitly bears out our expectation about the predictive potential of the INM mass model.

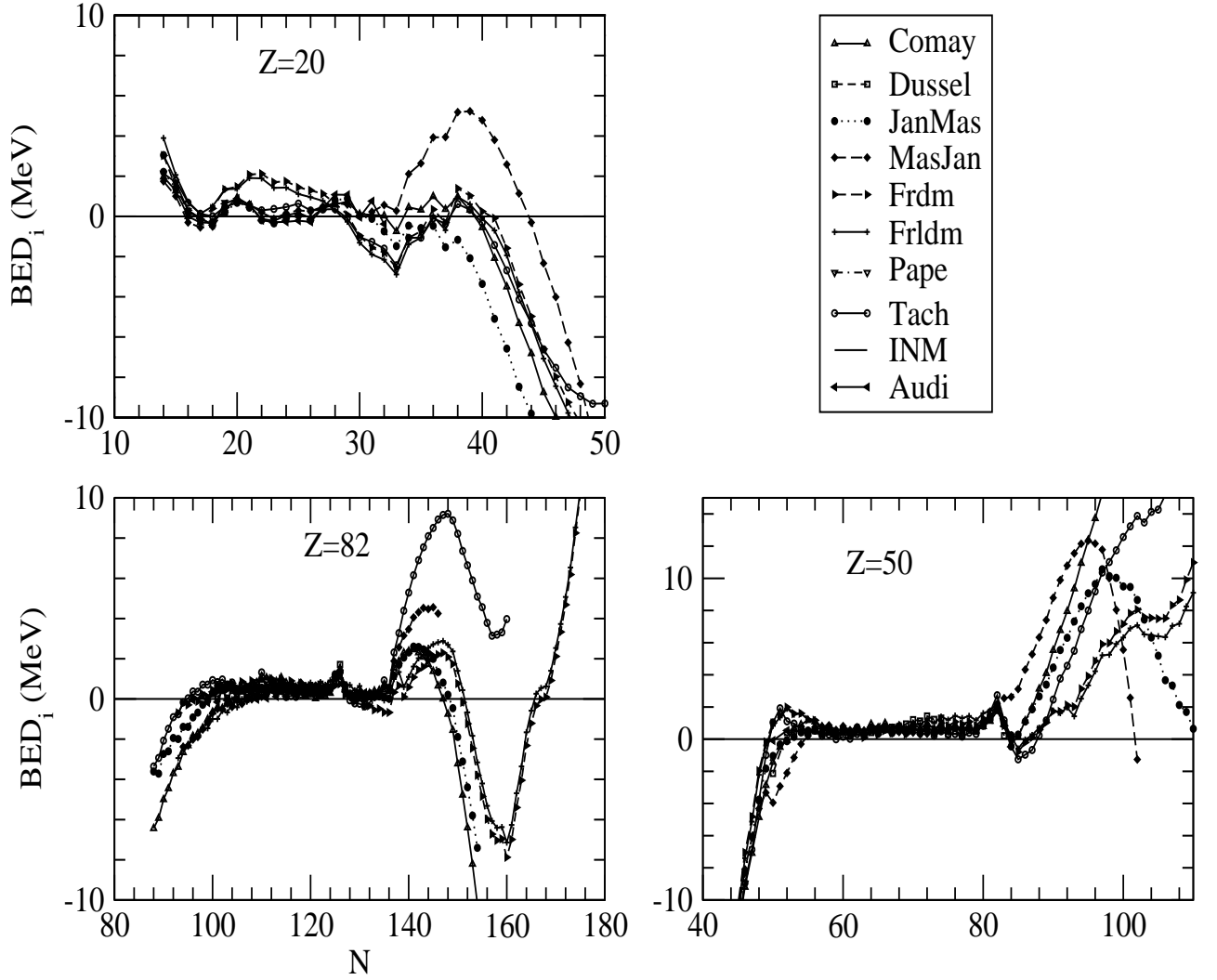


FIG. 9: Binding energy difference BED_i 's(Eq. 10) in Ca,Sn and Pb isotopes of various Mass Formula[16, 19] predictions with respect to those of the present INM predictions as the reference.

C. Shell Quenching in $N = 82$ and $N = 126$ Shells

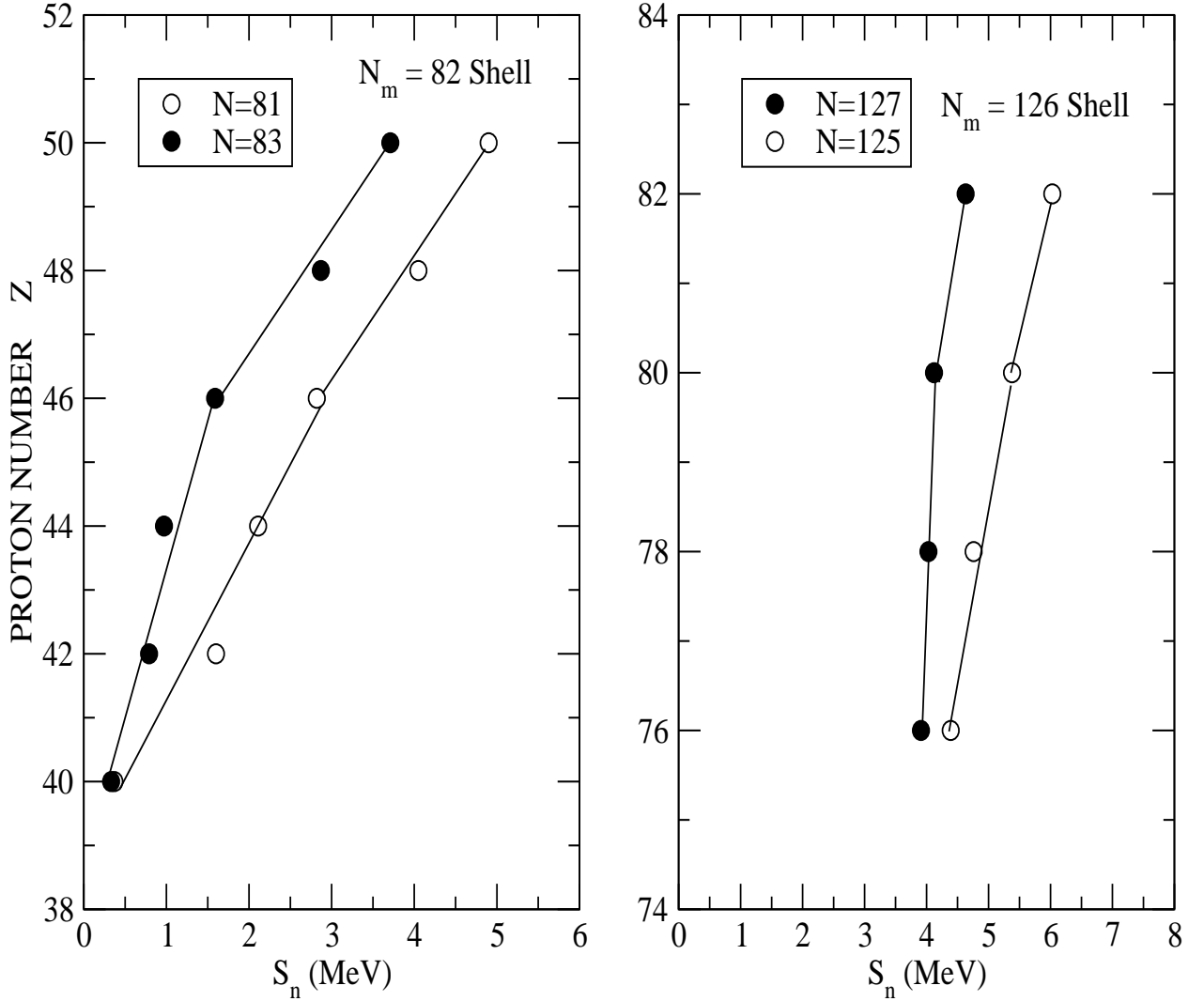


FIG. 10: Shell gaps given by $S_n(N_m - 1, Z) - S_n(N_m + 1, Z)$ for $N_m=82$ and 126 for various proton number Z showing shell-quenching in $N=82$ and 126 shells.

The shell structure is a very fundamental feature in nuclei. It plays a crucial role in building of different models for their description. In the valley of stability occurrence of well-defined shell structure in the form of magic numbers is well established and extensively

studied. In the INM model the same feature is also seen in the systematics of local energy η when these are plotted as isolines as shown in Fig. 5. One can clearly see such sharp-peaked Gaussian structures at the neutron magic numbers 50, 82 and 126. In general, whether such features persist in the unknown regions far from stability is of great current interest. Mass measurements of neutron-rich nuclei in the light and medium heavy regions have shown[23] that $N = 20$ shell gap vanishes for nuclei with $Z \leq 12$. Such shell quenching has also been seen for the $N = 50$ shell[24]. It is hoped that this phenomenon should also be seen for $N = 82$ and 126 shells. However conclusive proofs presently are lacking as masses of the relevant nuclei lying in the drip-line region have not yet been measured in the laboratory. Analysis of the abundances of various elements in r -process nucleosynthesis is suggestive[25] of the quenching of $N = 82$ shell. Our 1999 mass predictions show[10, 26] quenching in $N = 82$, and $N = 126$ shells. The present mass predictions reaffirm the same more convincingly. In Fig. (10), the shell gaps calculated using the present mass predictions are shown for $N = 82$ and $N = 126$ shells. Gradual vanishing of the gaps in both the cases are seen as one moves towards the drip-line regions.

D. Islands of Inversion

Neutron-rich nuclei lying in the proximity of the n-drip line are expected to show some exotic features in nuclear structure with dramatic departures from the normal trends observed in the β -stable valley. A well-known phenomenon having such a feature termed as 'island of inversion' has been observed[27] in neutron-rich nuclei around $N=20$ region quite early, which manifests in enhanced binding of those nuclei centering around ^{31}Na . It has been always a challenge to mass formulas and other structure models to explain this phenomenon. Extensive theoretical and experimental studies[28, 29] carried out over the years have concluded that the $N=20$ shell-closure in this region is broken by the intruder states from the pf -shell, inducing strong collectivity giving rise to high deformation. This has resulted in enhanced binding for Na and nearby nuclides in this region. Therefore with the present mass predictions in the INM model, we have attempted to make a through search throughout the nuclear landscape to see if our masses can account for the above known island of inversion and also identify possible new such islands. With this view we have plotted the S_{2n} isolines for all the nuclides from $Z=7$ to 105 in Figs. 11-13. The typical

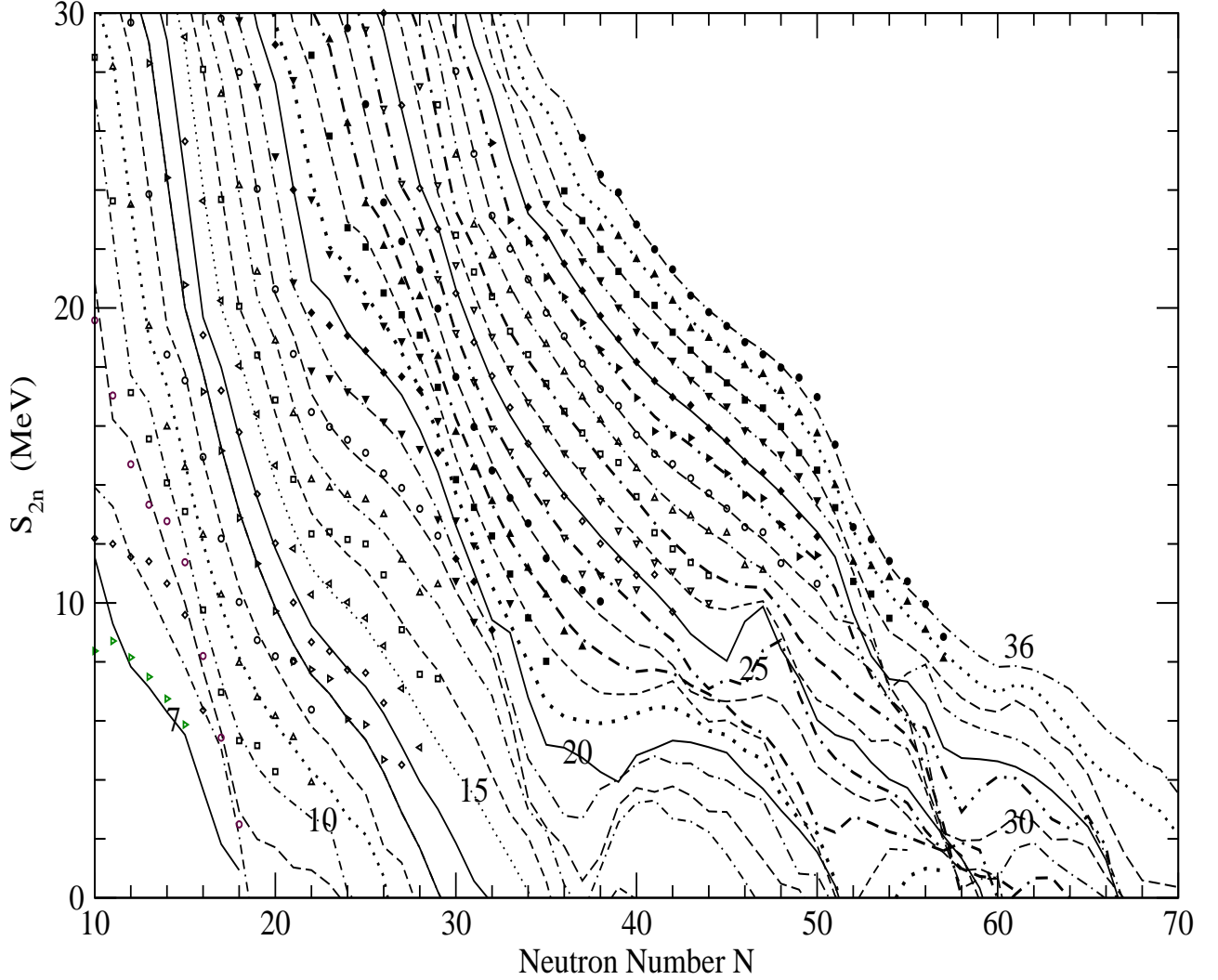


FIG. 11: The two-neutron separation energies S_{2n} as function of N for nuclei with $Z=7$ to 36 drawn as solid, broken, dash-dotted etc. lines. The corresponding Experimental[18] values where ever available are indicated by various symbols to distinguish the neighbouring isolines.

sharp fall of S_{2n} at the shell-closures clearly reproduce the well-known magic numbers 2, 8, 20, 50, 82 and 126 in conformity with experiment. However the monotonic decrease with increase of neutron numbers N in the β -stable valley gets arrested in the neutron-rich region

for $Z=10$ and 11 , agreeing with the observed island of inversion around ^{31}Na . Thus our mass predictions reproduce this feature reasonably well.

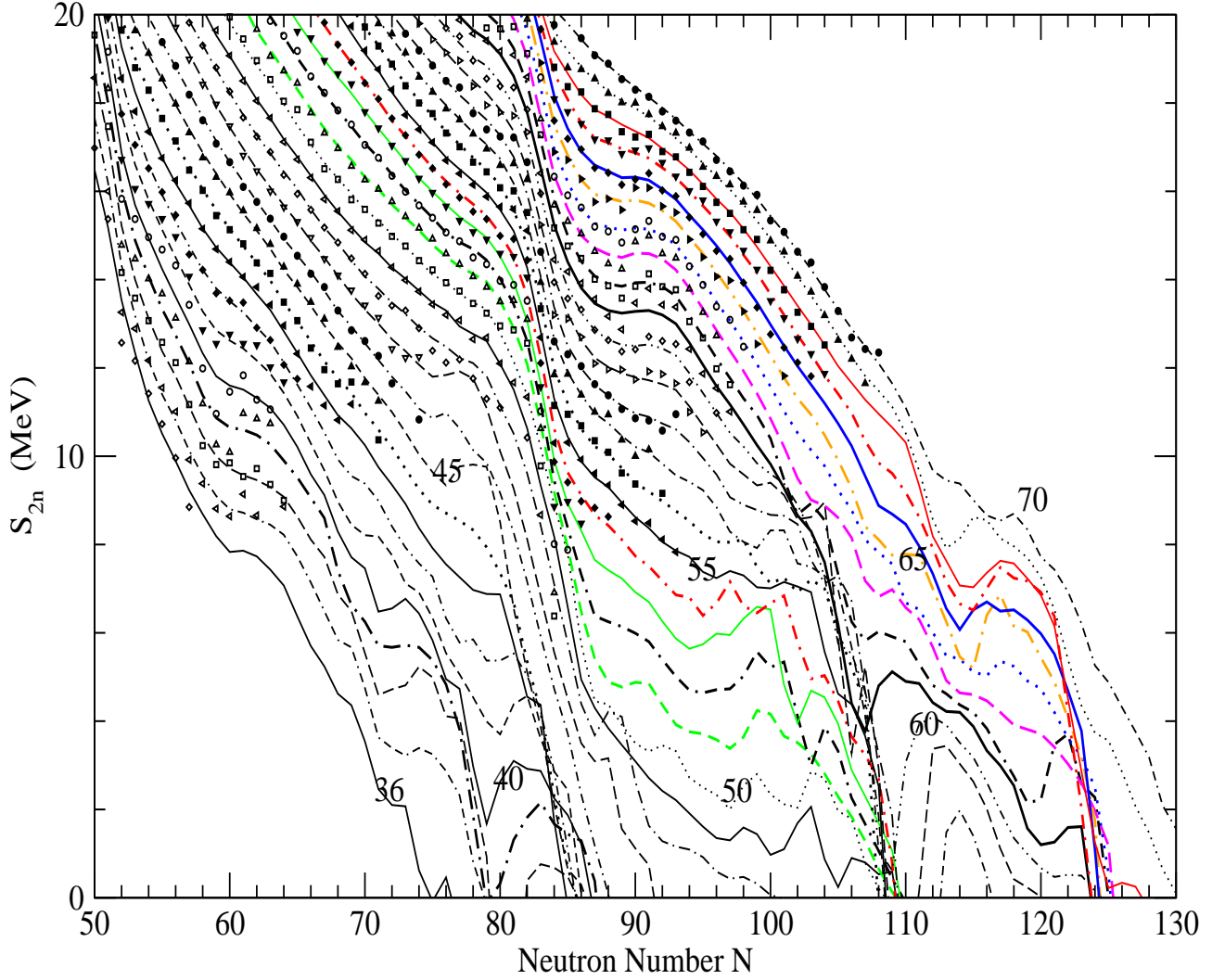


FIG. 12: Same as Fig.11 but for $Z=36$ to 70 .

It can also be seen in Fig. 11 that there is a region spanned by $Z=17$ to 23 and $N=38$ to 42 , where S_{2n} isolines exhibit the same feature of enhanced stability suggesting the existence of another island of inversion. This may originate due to breaking of $N=40$ shell by the intruder

states from the *sdg* shell and thereby inducing strong deformation. It is indeed satisfying to note that in the recent years strong evidences both theoretical and experimental have emerged[30, 31] supporting the existence of this island of inversion centering around ^{62}Ti . These two islands of inversion do suggest that these two may not be the isolated cases, and this phenomenon may be a general feature of nuclear dynamics in the exotic neutron-rich regions close to n-drip line, where breaking of shell- closures by intruder states from higher shells are highly plausible. In fact our extensive S_{2n} systematics in the high-mass region presented in Fig. 12 reveal two more islands in the heavy-mass region delineated by $Z=37-40$, $N= 70-74$; and $Z=60-64$, $N= 110-116$, where these may be due to breaking of $N=70$ and $N=112$ shells by the intruder states from the *pfh* and *sdgi* shells respectively.

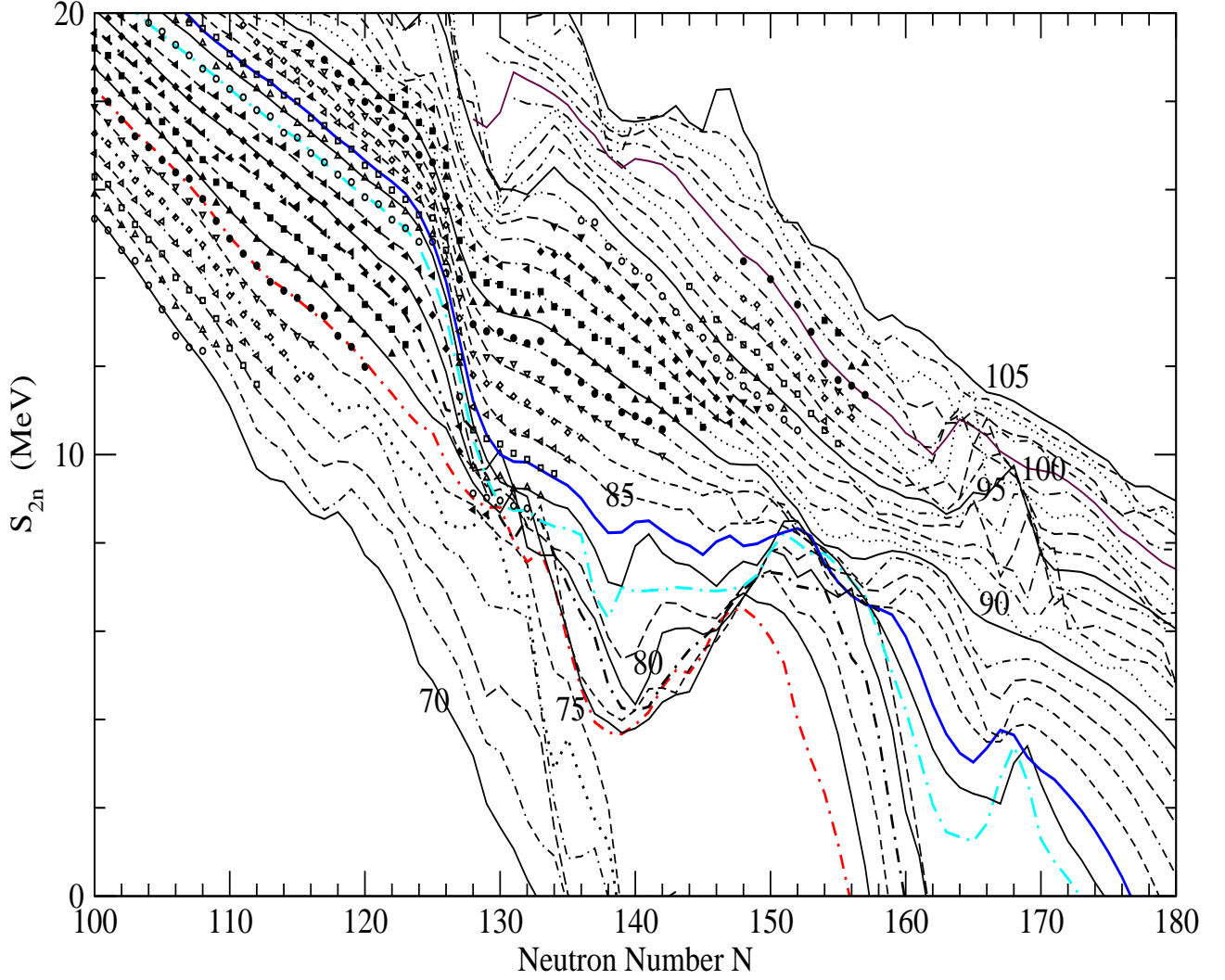


FIG. 13: Same as Fig.11 but for $Z= 70$ to 105 .

V. CONCLUSION

The Infinite Nuclear Matter model of atomic nuclei developed to its full potential over the last thirty years has been presented. The model has uncovered a new facet of the nucleus in which the nuclear matter characteristic has been revealed to be predominant. The abiding picture since the emergence of nuclear physics in 1930s is that the nucleus can be considered

as a classical liquid drop which formed the foundation of Bethe-Weizsaecker(BW) mass formula and its more refined version like the droplet model etc. These liquid drop based models are traditionalally used to define infinite nuclear matter and its saturation properties, determinable from nuclear masses. This has lead to many ambiguities and inconsistencies like r_0 -paradox, indeterminability of incompressibility etc. In contrast, the INM model has replaced the classical liquid by a quantum mechanical many-fermionic liquid which is the true nature of nuclear matter composed of the nucleus, by founding it on the generalized HVH theorem of many-body theory. Thus the liquid and the shell features, the two main features of nuclear dynamics could be taken into account non-perturbatively at the microscopic level. The model has succeeded in seperating the energy of the nucleus into a universal part represented by a sphere made up of infinite nuclear matter common to all nuclei, and a charecteristic part η called the local energy which varies from nucleus to nucleus. The universal part is described by only four parameters charecteristic of the nuclear matter and η being determined from nuclear masses through the solution of a differential equation of the model.

The effect of three-body has been included inadvertently by the use of HVH theorem, which is valid for such forces. Because of this proper physics input, the saturation density of nuclear matter could be obtained from nuclear masses in agreement with the value determined from electron-scattering on heavy nuclei, and thereby resolving the long standing r_0 -paradox. The energy per nucleon E/A of nuclear matter at ground-state has been consistently obtained from nuclear masses also. Thus both the saturation properties of nuclear matter E/A and ρ_∞ are obtained from the same source using the INM model. The third property of INM, namely the Incompressibility could be determined in more or less model independent manner using the same mass data that includes nuclear masses, and neutron and proton Fermi energies. Thus the data used for the determination of all the three saturation properties numbering about 4000, are well-respected as the most precision data in nuclear physics and that too pertaining to ground-state only.

The mass formula based on the INM model has the unique feature that it is formulated in terms of differential equations and thereby imbued with the ability for prediction of masses in unknown region. The root mean square deviation and the mean deviation of the mass-fit to 2198 known masses yields respectively 342 keV and 1.3 keV only the lowest in literature.

The model has introduced in nuclear physics a new entity, namely, the local energy η . It

contains all the characteristic properties like shell, deformation, diffuseness etc and therefore exceeds in scope compared to the usual shell-effect introduced by Strutinsky. In known regions, it is determined from experimental mass, and in unknown regions it is predicted by solution of a differential equation using the known ones as boundary conditions. The former being unique is endowed with the predictive potential, whereas the latter depending on the chosen meanfield is deficient in this respect. The systematics of η reveals new magic numbers in exotic neutron-rich nuclei in the dripline regions of the nuclear chart. This predictive ability is not contained in the usual shell effects, the latter being dependent on mean field which varies from interaction to interaction. The systematics of η predicts three islands of stability with $N=100$, $Z=62$; $N=150$, $Z=50$ and $N=164$, $Z=64$ around ^{162}SM , ^{228}Pt and ^{254}Th supported through microscopic studies in the framework of RMF theory and Strutinsky shell-correction calculation. This reveals a new effect in nuclear physics, where shell overcomes the instability due to repulsive components (triplet-triplet, singlet-singlet) of nuclear force, analogues to the superheavy elements where repulsive Coulomb instability is stabilized by the same, while the latter effect elongates the stability peninsula the former broadens it.

In comparative global analysis of all the mass models, the unique predictive ability of the INM mass model has been established by using its predicted binding energies as the reference and studying the systematics of the predicted masses of other mass models.

The shell-quenching in $N=82$ and 126 shells have been found using the INM masses, much anticipated but not predicted by any other mass models

The model has also shown the existence of new islands of inversion delineated by $Z=37-40$, $N=70-74$; $Z=60-64$, $N=110-116$; thus showing that the phenomenon is quite general and not confined to the well-known islands of inversion around ^{31}Na for a long time in nuclear physics. Thus in this respect, the INM model has been singularly successful.

The unique features of the INM mass model are:

- i) It does not use any effective interaction in any way, and thereby it is free from the vagaries of the uncertainty and from region to region variation.
- ii) It uses only the nuclear masses and Fermi energies determined solely by experiment.
- iii) It takes into account three-body, and other multibody forces (if present) in nuclei.

4) It is built in terms a differential equation and thus equipped with physics for prediction.

The distinctive success of the INM model may be attributed to these features.

-
- [1] J. Decharge and D. Gogny, Phys. Rev. C **21**, 1568 (1980).
- [2] J. M. Pearson, Phys. Lett. **B91**, 325 (1980); J. M. Pearson, Nucl. Phys. **A376**, 501 (1982);
F. Tondeur, J. M. Pearson and M. Farine, Nucl. Phys. **A394**, 462 (1983).
- [3] L. Satpathy, J. Phys. **G13**, 761 (1987).
- [4] L. Satpathy and R. C. Nayak, Phys. Rev. Lett. **51**, 1243 (1983).
- [5] L. Satpathy and R. C. Nayak, ATOMIC DATA AND NUCLEAR DATA TABLES, **39**, 213 (1988).
- [6] R. C. Nayak and L. Satpathy ATOMIC DATA AND NUCLEAR DATA TABLES, **73**, 213 (1999).
- [7] N. H. Hugenholtz and W. Van Hove, Physical (Utrecht) **24**, 363 (1958).
- [8] R. C. Nayak, V. S. Uma Maheswari and L. Satpathy, Phys. Rev. C **52**, 711 (1995)
- [9] L. Satpathy, V. S. Uma Maheswari and R. C. Nayak, Phys. Rep. 319, 85(1999)
- [10] R. C. Nayak, Phys. Rev. C 319, 85(1999)
- [11] L. Satpathy and S. K. Patra, J. Phys. **G30**, 771(2004).
- [12] W. Mittag, P. Roussel-Chomaz and A.C.C. Villari, Europhys. News **35**, No. 4(2004)(<http://www.europhysicsnews.com/full/28/article3/article3.html>)
- [13] NuPECC Reort "Nuclear Physics in Europe: Highlights and Opportunities" (1997)(<http://www.nupecc.org/nupecc/report97/report97final/node6.html>)
- [14] J. Billowes *et al.*, SIRIUS Science, CLRC ISBN 0-90376-75-6, December 1998 (<http://marie.surrey.ac.uk/upg/sirius/SIRIUSver3.pdf>)
- [15] S. K. Patra, P. Arumugam and L. Satpathy, Bulletin Board Nucl-th/ 0504063
- [16] P. Möller, J. R. Nix, W. D. Myers and W. Swiatecki, ATOMIC DATA AND NUCLEAR DATA TABLES, **59**, 185 (1995)
- [17] P. Möller, W. D. Myers, W. Swiatecki and J. Treiner, ATOMIC DATA AND NUCLEAR DATA TABLES, **39**, 225 (1988)
- [18] G. Audi, A. H. Wapstra and C. Thibault, Nucl. Phys. **A729**, 337 (2003).
- [19] P. Haustein, Atomic Data and Nuclear Data Tables **39**, 185(1988)(<http://ie.lbl.gov/toimass.html>)

- [20] J. Duflo and A. Zucker, Phys. Rev. **C 52**, R23(1996)
- [21] G. A. Lalazissis, J. Koenig and P. Ring, Phys. Rev. **C55**, 540(1997)
- [22] G. A. Lalazissis, S. Raman and P. Ring, Atomic Data and Nuclear data Tables **71**,1 (1999)
- [23] N. Fukunishi, T. Otsuka and T. Sebe, Phys. Lett. **B96**, 279 (1992).
- [24] K.-L. Kratz *et al.* Astrophysics J. **403**, 216 (1993).
- [25] B. Chen *et al.*, Phys. Lett. **B355**, 37 (1995).
- [26] L. Satpathy and R. C. Nayak, J. Phys. **G24**, 1527 (1998).
- [27] C. Thibault *et al.*, Phys. Rev. **C 12**,644 (1975)
- [28] X. Campi *et al.* Nucl. Phys. **A251**, 193 (1975).
- [29] E. K. Warburton, J. A. Becker and B. A. Brown, Phys. Rev. **C 41**, 1147 (1990)
- [30] O.B. Tarasov *et al.*, Phys. Rev. Lett. **102**(2009) 142501, Science Daily Feb.3 (2011).
- [31] S. M. Lenzi *et al.*, Phys. Rev. **C 82**, 054301(2010)

VI. EXPLANATION OF TABLE

VII. TABLE

Calculated Nuclear Ground-State Binding Energies and Mass Excesses, Compared to Experimental Mass Excesses Where Available along with One-neutron, Two-neutron, One-proton and Two-proton, α -particle Separation Energies

Z	Proton number. The mass table is ordered by increasing proton number. The corresponding name of each element is given in parenthesis.
N	Neutron number.
A	Mass number.
BE(MeV)	Calculated binding energy $B(N,Z)$ of a nucleus (N,Z) using Eq. (3).
ME(MeV)	Calculated mass excess. Nuclei that are unstable against one-nucleon and two-nucleon decay are denoted by symbols (\dagger) and (\ddagger), respectively.
ME _{exp} (MeV)	Experimental mass excess of Audi-Wapstra[18].
Err (Mev)	The error associated with the Experimental mass excess[18].
$S_n(MeV)$	Calculated One-neutron Separation Energies given by $B(N,Z)-B(N-1,Z)$.
$S_{2n}(MeV)$	Calculated Two-neutron Separation Energies given by $B(N,Z)-B(N-2,Z)$.
S_p (MeV)	Calculated One-proton Separation Energies given by $B(N,Z)-B(N,Z-1)$.
S_p (MeV)	Calculated Two-proton Separation Energies given by $B(N,Z)-B(N,Z-2)$.
S_α (MeV)	Calculated α -Particle Separation Energies given by $B(N,Z)-B(N-2,Z-2)-28.296$.